

This is the final peer-reviewed accepted manuscript of:

Perspectives on protein biopolymers: miniaturized flow field-flow fractionation-assisted characterization of a single-cysteine mutated phaseolin expressed in transplastomic tobacco plants

Marassi V.; De Marchis F.; Roda B.; Bellucci M.; Capecchi A.; Reschiglian P.; Pompa A.; Zattoni A.

Journal of Chromatography A

Volume 1637, 25 January 2021, 461806

The final published version is available online at:

<https://doi.org/10.1016/j.chroma.2020.461806>

Terms of use:

Some rights reserved. The terms and conditions for the reuse of this version of the manuscript are specified in the publishing policy. For all terms of use and more information see the publisher's website.

This item was downloaded from IRIS Università di Bologna (<https://cris.unibo.it/>)

When citing, please refer to the published version.

1 **Perspectives on protein biopolymers: miniaturized flow field-flow fractionation-assisted**
2 **characterization of a single-cysteine mutated phaseolin expressed in transplastomic tobacco**
3 **plants**

4

5 Valentina Marassi^{1,4}, Francesca De Marchis², Barbara Roda^{1,4}, Michele Bellucci², Alice Capecchi²,
6 Pierluigi Reschiglian^{1,4}, Andrea Pompa³, Andrea Zattoni^{1,4*}

7

8

9 *1. Department of Chemistry G. Ciamician, University of Bologna, Bologna, Italy*

10 *2. Institute of Biosciences and Bioresources—Research Division of Perugia, National Research*
11 *Council of Italy, via della Madonna Alta 130, 06128, Perugia (PG), Italy*

12 *3. Department of Biomolecular Sciences, University of Urbino "Carlo Bo", via Donato Bramante 28,*
13 *61029 Urbino (PU), Italy*

14 *4. byFlow srl, via dell'Arcoveggio 74, 40128 Bologna (BO), Italy*

15 ** corresponding author, andrea.zattoni@unibo.it*

16

17 **HIGHLIGHTS**

18

- 19 - Transplastomic phaseolin (P*) expressed in tobacco thylakoids could be exploited in the
20 production of biopolymers
- 21 - Plant extracts were submitted to hollow fiber flow field flow fractionation coupled to multi-
22 angle light scattering (HF5-MALS) with two separation methods
- 23 - Characterization of native phaseolin and P* showed differences in aggregation state and molar
24 mass
- 25 - Conformation studies confirm the concatenation of P* into elongated forms compatible with
26 successful polymerization

27

28 **KEYWORDS**

29

30 hollow fiber flow field flow fractionation

31 multi-angle light scattering

32 protein biopolymers

33 transplastomic phaseolin

34 **ABSTRACT**

35

36 The development of plant-based protein polymers to employ in biofilm production represents the
37 promising intersection between material science and sustainability, and allows to obtain
38 biodegradable materials that also possess excellent physicochemical properties. A possible candidate
39 for protein biopolymer production is phaseolin, a storage protein highly abundant in P Vulgaris beans.
40 We previously showed that transformed tobacco chloroplasts could be employed to express a mutated
41 phaseolin carrying a signal peptide (directing it into the thylakoids) also enriched of a cysteine residue
42 added to its C-terminal region. This modification allows for the formation of inter-chain disulfide
43 bonds, as we previously demonstrated, and should promote polymerization.

44 To verify the effect of the peptide modification and to quantify polymer formation, we employed
45 hollow-fiber flow field-flow fractionation coupled to UV and multi-angle laser scattering detection
46 (HF5-UV-MALS): HF5 allows for the selective size-based separation of phaseolin species, whereas
47 MALS calculates molar mass and conformation state of each population. With the use of **two different**
48 **HF5** separation methods we first observed the native state of P.Vulgaris phaseolin, mainly assembled
49 into trimers, and compared it to mutated phaseolin (P*) which instead resulted highly aggregated.
50 Then we further characterized P* using a second separation method, discriminating between two and
51 distinct high-molecular weight (HMW) species, one averaging 0.8×10^6 Da and the second reaching
52 the tens of million Da. Insight on the conformation of these HMW species was offered from their
53 **conformation plots**, which confirmed the positive impact of the Cys modification on polymerization.

54

55 1. INTRODUCTION

56 Proteins are organic heteropolymers serving as nutrients and structural compounds in living
57 organisms with also important roles in cell function and regulation. They generally exist in nature
58 either in the form of insoluble fibrous proteins or water-soluble globular proteins. Their broad
59 spectrum of functional and structural properties due to polar and nonpolar amino acids make them
60 promising raw materials for the production of bioplastics used for packaging materials. Biodegradable
61 polymers (biopolymers) derived from renewable natural resources to produce bioplastics is thus a
62 research topic of growing interest [1]. At present, a number of protein-based films are produced for
63 food packaging [2]. Indeed, they show excellent optical properties (gloss and transparency), are good
64 fat barriers, at low and intermediate humidity feature an excellent oxygen and organic vapor barrier
65 and have fair mechanical properties [3].

66 The plant polypeptide phaseolin accounts for 50% of the total seed protein of the leguminous species
67 common bean, *Phaseolus vulgaris* L.[4], which is one of the most commonly produced and consumed
68 food legume worldwide, especially in Asia, South America and Africa [5]. This globulin protein
69 belongs to the vicilin (or 7S) family of seed storage proteins and is a homotrimeric glycoprotein.
70 Phaseolin monomer has a weak internal duplication constituted by two regions with a similar
71 secondary structure, each region made up of a β -barrel domain followed by a α -helical cluster
72 comprising of three helices. The trimer is composed of three similar polypeptides linked mainly by
73 hydrophobic interactions between two α -helical clusters [6, 7]. Phaseolin is encoded by a small gene
74 family and consists of two highly homologous classes of α - and β -polypeptides of molecular weight
75 around 45 – 46 kDa, after that their N-terminal, 24-aminoacid signal peptide is cleaved inside the
76 endoplasmic reticulum [8]. In view of its excellent functional properties [9], phaseolin can be applied
77 in food formulations [10], or fused to proteins of biotechnological interest [11], but its potential can
78 also be explored for the production of protein biopolymers.

79 One way to obtain biopolymers from plant proteins is to exploit the protein synthesis mechanisms of
80 the plant itself. Transformation of the chloroplast genome (plastome) has been largely used for the
81 production of heterologous proteins [12] [13], including protein biopolymers [14] [15]. Therefore, in
82 this study, we transformed tobacco plastome with a β -phaseolin gene in which a cysteine residue has
83 been added to the C-terminal region. This single insertion is able to allow the formation of phaseolin
84 inter-chain disulfide bonds because the cysteine residue is not hidden in the phaseolin trimers but
85 remains exposed, thus enabling the formation of disulfide bonds among trimers [16]. The β -phaseolin
86 gene has been chosen because the crystal forms used to investigate the phaseolin three-dimensional
87 structure showed only β -polypeptides [6]. Moreover, we previously demonstrated that β -phaseolin
88 signal peptide targets a recombinant phaseolin protein to the thylakoid membrane when it is expressed

89 in tobacco chloroplasts. Indeed, thylakoid localization increases the possibility to produce phaseolin
90 polymers because, in the oxidative environment of this chloroplast sub-compartment, recombinant
91 phaseolin trimers can form higher order systems through disulfide bonds [17]. Moreover, thylakoid-
92 targeted phaseolin can avoid an autoregulatory mechanism which inhibits its mRNA translation [18].
93 To verify the potential of the thylakoid compartment for phaseolin polymer production it is necessary
94 to assess whether the extracted protein matter consists of phaseolin polymers, oligomers, or both: this
95 implies that in the case of a heterogeneous extract, MW/size-based separation of protein components
96 is necessary. Separation should also be coupled to characterization techniques able to weigh the
97 species found, to provide information on the aggregation/polymerization state.

98 Flow field-flow fractionation (F4) is one of the most performing size-separation techniques: together
99 with size-exclusion chromatography (SEC), it is the benchmark technique for protein and antibody
100 size characterization and is suggested by FDA as a technique that complements SEC in the validation
101 of protein products [19]. F4 is a flow-assisted technique ideally suited to size-separate dispersed
102 analytes over a broad size range [20]: in F4 retention time is inversely proportional to the
103 hydrodynamic diffusion coefficient of the analyte and, consequently, it is directly proportional to its
104 hydrodynamic size. The analyses can be performed in physiological conditions, allowing for the
105 separation and detection of delicate species in native conditions [21, 22], [23] [24]. The most used F4
106 technique is Asymmetrical F4 (AF4), where the sample is separated in a flat capillary channel with a
107 porous wall generating the hydrodynamic field.

108 Flow-based separation science applied to food and agricultural chemistry proved its efficacy on a
109 variety of analytes such as polysaccharides from grains [25] and fungi [26], beer proteins [27], wine
110 [28] [29] and even intact plant ribosomes [30].

111 In the first stages of biomaterial development it is desirable to be able to work with a low amount of
112 starting material, to facilitate production optimization prior to larger-scale development. This is the
113 case with phaseolin polymerization into chloroplast compartments where separation and
114 characterization efficacy should meet with a reduced-volume working environment

115 The microvolume variant of F4, HF5, merges the advantages of such a technique with a lower sample
116 volume and demonstrated to be a successful alternative to SEC [31]: down-scaling of the separation
117 channel is advantageous for application in the bio-pharmaceutical field and to give insight during
118 protocol development, since the lower injection volume makes it possible to work samples such as
119 small amounts of plant extracts. Lastly, disposable usage of the separating channel eliminates sample
120 carry-over or sample contamination issues [32] [33] [34] [35]. HF5 has proved its potential in the
121 characterization of complex protein samples, monitoring of protein drug aggregation, and even
122 monitoring of time-dependent formation of amyloid fibrils [24] [36] [37, 38], but had not breached

123 into the field of plant/food chemistry up to now. When online coupled to uncorrelated detection
124 methods such as MALS and spectrophotometric detectors, HF5 provides high-resolution size
125 distribution analysis. This platform is effective in the investigation of High MW **protein** species, since
126 it reduces the occurrence of artifacts, and can highlight the stability of oligomers and higher-order
127 aggregates. In the present work, to investigate the effective formation of phaseolin polymeric species,
128 phaseolin standard obtained from beans and transplastomic phaseolin extracted from tobacco leaves
129 were characterized and compared. To quantify and characterize the phaseolin polymers, we employed
130 hollow-fiber flow field-flow fractionation (HF5) coupled to UV absorption and multi-angle light
131 scattering (MALS) detection.

132

133

134

135

136

2. MATERIALS AND METHODS

2.1 Gene constructs and plant transformation.

Beta phaseolin cDNA gene was amplified from plasmid pDHA.T343F [39] with NdeI-P (5'-tccatcggacatatgatgagagca-3') and NotI-P*(5'-ccccctccggatcgcgccgctagtacacaaat**gcaccctttcttcct**-3') oligonucleotides to introduce a *NdeI* and a *NotI* restriction site (underlined) at the 5' and 3' ends of the gene, respectively. Moreover, primer NotI-P* is designed to insert a cysteine residue (in bold) at the C-terminal of the protein to allow inter-chain disulphide bridge formation. The PCR product was digested with *NdeI/NotI* and cloned into pCR2.1-5'UTR[40], to obtain the pCR2.1- 5'UTR-P* intermediate plasmid, in which phaseolin is under the control of the plastidial *psbA* promoter/5'UTR. The *psbA/5'UTR-P** cassette was excised from pCR2.1-5'UTR-P* by *EcoRV/NotI* digestion and subcloned into pLD-CTV tobacco plastid vector [41], generating pLD-CTV-P*. Homoplasmic transplastomic plants were obtained by particle bombardment into tobacco leaves of gold microprojectiles coated with pLD-CtV-P* as described [42]. Transplastomic plants were grown at 25°C in 16 h of light in axenic conditions before being transferred to the greenhouse for seed production.

2.2 Phaseolin analysis.

Phaseolin purification: Phaseolin (P) purification was performed from *P. vulgaris* L. seeds (variety small red) according to Suzuki and colleagues [43] with minor modifications. **All reagents used were of analytical grade and were obtained from Merck KGaA, Darmstadt, Germany. All solutions were prepared with deionised water having a conductivity of <1 µS/cm.** After acidic extraction, the protein was further purified by velocity centrifugation on Sucrose gradient. One ml of phaseolin extract was loaded on a 13 mL linear 5% to 25% (w/v) Sucrose gradient made in 150 mM NaCl, 1 mM EDTA, 0.1% Triton X-100, 50 mM Tris-Cl, pH 7.5. After centrifugation at 110,000 g overnight at 4° C, the fractions containing phaseolin, corresponding to those where proteins of about 150 kDa are localized, were collected and merged. To verify purity of the phaseolin extract, an aliquot of this pool was analyzed by SDS-PAGE followed by Western blotting with anti-phaseolin antibody (1:10,000) as described [44]. The merged fractions containing phaseolin were dialyzed for 3 days in distilled H₂O, lyophilized and finally resuspended at a concentration of 3 mg/ml in PBS.

Single cystein-mutated phaseolin (P) analysis and extraction from transplastomic plants:* Total leaf proteins were extracted from 0.3 g of tissues from transplastomic plants, grounded in liquid nitrogen, homogenized in 0.8 mL of extraction buffer (200 mM NaCl, 1 mM EDTA, 0.2% Triton X-100, 100

170 mM Tris-Cl, pH 7.8) supplemented with 'Complete' protease inhibitor cocktail (Merck) and analysed
171 by Western blotting as described above.

172 For P* purification, one hundred and fifty grams of transformed tobacco young leaves were collected
173 after being let in the dark overnight to prevent starch accumulation. They were grinded in a blender
174 with 1.5 L of grinding buffer (GB: 0.33 M sorbitol, 0.2 M Hepes, 0.1 M EDTA, 0.2 M MgCl₂, 1 mM
175 2-Mercaptoethanol, 4.4 mM isoascorbic acid, pH 6.8) four times at low speed for 10 sec each time.
176 The homogenate was filtered through a layer of Miracloth paper and four layers of gauze before
177 centrifugation at 1,700 g for 2' at 4°C. The supernatant was discarded and the pellet, containing both
178 broken and intact chloroplasts, was solubilized in the extraction buffer (EB: 0.2 M NaCl, 2% Triton
179 X-100, 1 mM EDTA, 0.1 M Tris-Cl, pH 7.8, supplemented with Complete protease inhibitor cocktail)
180 to dissolve chloroplasts membranes. To remove residual starch an additional centrifugation at 14,000
181 g for 5' at 4°C was performed. Three hundred µL of the resulting supernatant were loaded on a 13
182 mL velocity Suc gradient 5% - 25% (w/w) made in 150 mM NaCl, 1 mM EDTA, 0.1% Triton X-100,
183 50 mM Tris-Cl, pH 7.5. After centrifugation at 110,000 g, for 24 h at 4°C, 18 fractions of about 0.8
184 mL and the sample pelleted at the bottom of the tube were collected. An equal aliquot of each fraction
185 and the pellet was analyzed by SDS-PAGE and Western blot with anti-phaseolin antiserum as
186 described above. According to the Western blot results, the bottom of the tube was recovered with 1
187 mL of distilled H₂O, dialyzed, lyophilized, resuspended in isotonic, pH 7.4 PBS at 0.3 mg/mL and
188 analysed by HF5-MALS. Considering that the initial concentration of P* in the leaves is 0.5% of the
189 total soluble protein, we calculated the P* extraction efficiency which is around 53%.

190

191 2.3 HF5-UV-MALS.

192 HF5 analyses were performed using an Agilent 1200 HPLC system (Agilent Technologies, Santa
193 Clara, CA, USA) consisting in a degasser, an isocratic pump, with an Agilent 1100 DAD UV/Vis
194 spectrophotometer combined with an Eclipse® DUALTEC separation system (Wyatt Technology
195 Europe, Dernbach, Germany). The hollow fiber was a polyethersulfone (PES) fiber, type FUS 0181
196 available from Microdyn-Nadir (Wiesbaden, Germany) with the following characteristics: 0.8 mm
197 ID, 1.3 mm OD, and 10 kDa Mw cut-off, corresponding to an average pore diameter of 5 nm. The
198 HF5 channels used for the experimental section were standard cartridges containing a 17 cm long
199 fiber, commercially available. The scheme of the HF5 cartridge, its assembly and the modes of
200 operation of the Eclipse® DUALTEC system have already been described elsewhere[33]. The
201 ChemStation version B.04.02 (Agilent Technologies) data system for Agilent instrumentation was
202 used to set and control the instrumentation and method parameters. The software package Wyatt
203 Eclipse @ ChemStation version 3.5.02 (Wyatt Technology Europe) was used to set and control the

204 flow rate values. A 3-angle multi-angle light scattering detector model miniDAWN TREOS (Wyatt
205 Technology Corporation, Santa Barbara, CA, USA) operating at a wavelength of 658 nm, was used
206 to measure the radius and molar mass of particles in suspension, with the software ASTRA® version
207 6.1.7 (Wyatt Technology Corporation). **Analyses were carried out in isotonic, pH 7.4 PBS as mobile**
208 **phase.** An HF5 conventional method is composed of four steps: focus, focus–injection, elution and
209 elution–injection. During the focus, the mobile phase is split into two different streams entering from
210 inlet and outlet; during focus–injection, the flow settings remain unvaried while the sample is
211 introduced into the channel through the inlet and focused in a narrow band. Then, in the elution step,
212 the flow of mobile phase enters the channel inlet and it splits in a radial component which exits the
213 fiber’s pores (cross-flow), and a longitudinal component (channel flow, V_c) that reaches the detectors.
214 Lastly, during elution–injection, no cross-flow is applied and any remaining sample inside the channel
215 is released; also, the flow is redirected in the injection line as well to clean it before the next injection.
216 Longitudinal flow is indicated as V_c , while cross/focus flow as V_x . The two different separation
217 methods developed in this work are summarized in Table 1.

218 Due to the parabolic flow profile of the carrier flow, smaller particles experience higher flow rates
219 (on the average) than larger ones. In this normal fractionation mode, the particle retention is a function
220 of its apparent diffusion coefficient. Hence, the particle retention volume can be related to its diffusion
221 coefficient, and consequently, to its hydrodynamic diameter (D_h) or radius (R_h) using the Stoke’s
222 equation. The conversion of the retention volume to hydrodynamic radius/molar mass can be
223 accomplished by calculating channel parameters and applying F4 theory: in our work, the software
224 ISIS (Wyatt Technology Europe), allowed us to calculate the expected retention times of proteins
225 eluting under an input method, accounting for membrane swelling, ionic strength and instrumental
226 parameters. FIFFF theory rigors are described elsewhere[45]. Multi-angle light scattering (MALS)
227 was used to calculate the molar mass of eluted proteins **after normalization with standard bovine**
228 **serum albumin monomer.** MALS allows for the absolute determination of particle root mean square
229 radius of gyration (R_g) by measuring the net intensity of light scattered by such particles at a range
230 of fixed angles, and by consequence, knowing the dn/dc and absorptivity values of the analysed
231 species, the molar mass value of the eluting species[46]. The correlation between Radius of gyration
232 and molar mass distributions provides information on the particle conformation in suspension through
233 the calculation of a scaling exponent ν , or ν value. The ν value is the slope in a double logarithmic
234 $\log MW - \log R_g$ plot, and is theoretically defined for spheres as $\nu = 0.33$, random-coil $\nu = 0.5-0.6$,
235 and rod-like structures $\nu \sim 1$ [47] [48].

236

237

3. RESULTS AND DISCUSSION

3.1 Preparation of *P. Vulgaris* phaseolin and recombinant tobacco phaseolin

Lyophilized phaseolin (P) obtained from *P. vulgaris* was resuspended in PBS at a final concentration of 3 mg/mL, whereas the purified mutant phaseolin (P*) had a concentration of 0.3 mg/mL in PBS. P localization in the bean seed cells depends on the presence of two sorting signals: a N-terminal 24 amino acid signal peptide (SP), and a C-terminal four-amino acid propetide (AFVY). The first allows the post-translational insertion of P polypeptides from the cytoplasm into the endoplasmic reticulum (ER), while the second directs P polypeptides from the ER to vacuoles. Since genetically modified tobacco plants undergo insertion of the P* recombinant gene in the plastome, P* is synthesized inside the chloroplast stroma and the SP directs this mutated phaseolin, with a cysteine residue added to the C-terminal, to the thylakoid compartment (Figure 1) [16] [17].

3.2 Gel electrophoresis

Purified bean P, as expected [8] [49], is detected by SDS-PAGE followed by Coomassie staining as several differentially glycosylated monomers of α - and β -polypeptides of molecular weight around 45 – 50 kDa (Figure 2A). Western blot analysis with the anti-phaseolin antiserum confirms the specificity of these polypeptides (Figure 2A). Conversely, the modified P* sample purified from chloroplasts of transplastomic tobacco leaves, when analyzed by Western blot, shows a pattern formed by different phaseolin polypeptides. Apart from the expected unglycosylated 45-kDa polypeptide (the enzymes for glycosylation are not present inside the chloroplast), additional P* forms, not detected in the P sample, are a dimer, with an apparent molecular mass of around 83 kDa, and higher molecular mass forms (Figure 2B). The 83-kDa dimers derive from disulfide bonds between P* monomers (Pompa et al. 2010), while the P* aggregates around 100 – 180 kDa are unexpected. At physiological pH, the most stable form of bean P is thought to be trimeric, with 46 kDa polypeptide being the protomer [50], thus it is likely that these superstructures are denatured in SDS-PAGE followed by Western blotting (Figure 2B). This is only in part true for P*, whose polypeptide species around 100 – 180 kDa are prevalent, suggesting that P* mainly consists in stable, heavier species (Figure 2B).

SDS denaturation does not provide a truthful characterization of the samples content. However, the presence of P* monomers and oligomers confirms the presence of P* polypeptides localized in the chloroplast thylakoids in different forms [17]. To carry out a more in-depth evaluation of the P* high molecular mass species, chloroplasts from leaves of transplastomic tobacco plants have been isolated and then solubilized with a buffer containing 2% Triton X-100. The resulting homogenate was loaded on a velocity Sucrose gradient and the various fractions obtained were subjected to Western blot

272 analysis (Fig 3a). Almost all the P* protein was recovered in the bottom of the tube, confirming that
273 P* is localized in chloroplasts as polypeptides of molecular mass higher than 700 kDa. On the
274 contrary, the amount of trimeric P* is extremely low, as indicated by the very weak signals
275 corresponding to the components of the fractions 7 – 9 that migrated as a trimer, around 150 kDa (Fig
276 3b).

277

278 **3.3 HF5-UV-MALS Analysis**

279 To effectively estimate the size of phaseolin oligo/polymeric systems, we employed hollow fiber flow
280 field-flow fractionation coupled to UV and MALS detection.

281 To characterize phaseolin extracts, we developed a first separation method (Method 1) which was
282 able to resolve phaseolin aggregated states present in *P. vulgaris*. Then, the tobacco-derived protein
283 extract was submitted to the same method, but the protein species detected had a high-enough size to
284 be fully retained. Therefore, we switched to a second, softer **HF5 separation** method (Method 2) to
285 improve characterization, and compare these high-MW species to “standard” phaseolin in the same
286 conditions.

287

288 **3.3.1 Characterization of standard phaseolin extracted from *P. vulgaris***

289 Liophilized phaseolin was resuspended in PBS at 3mg/mL and 10 µL were analysed at t0 with
290 method 1. In Figure 4 the fractogram obtained is overlaid with the mass values calculated at peak
291 maxima.

292 Phaseolin was mainly present as its stable trimeric form (143 kDa), eluted at 16.5 minutes. The mass
293 calculated at 19 min (275 kDa) corresponds instead to phaseolin 6-mer. The third shoulder is
294 phaseolin 9-mer. By calculating the retention time expected for protein species in the developed
295 method (see Materials and Methods), we could also attribute the peak at 14 min to the dimer. The
296 relative abundance (expressed as % of the integration of the absorption signal at 280 nm) of each
297 species and their aggregation state attribution are shown in Table 2.

298 Even though at physiological pH phaseolin is mostly present at trimer, other aggregation states are
299 visible and separated, showing that phaseolin favours the formation of stable species with various
300 grades of assembly.

301

302 **3.3.2 Characterisation of phaseolin putative polymers extracted from transplastomic tobacco 303 plants**

304 The pellet of a velocity sucrose gradient (Fig 3), utilized to purify the modified phaseolin (P*)
305 extracted from transplastomic tobacco plants, was recovered, dialyzed and lyophilized. P * was

306 resuspended in PBS and subjected to Method 1. Given the lower concentration obtained (0.3 mg/mL
307 from Nanodrop measurements), the injection volume was increased to 50 μ L.
308 In the fractogram obtained (Figure 5), there is no evidence of phaseolin trimer and oligomers, apart
309 from a small band between 10 and 14 min. Instead, one single peak corresponding to high molecular
310 weight species is visible starting from 24 min and eluted in proximity and after the field release (at
311 25.5 min). Its molar mass distribution ranged from 10^6 to 10^7 Da showing that P* is differently
312 arranged than P: the presence of disulfide bond-prone residues seem in fact not only to promote higher
313 order accretion, but limits the ability to form lower order oligomers such as the expected trimer.

314

315 **3.3.3 Characterisation of the different polymer populations**

316 To better elucidate the actual size of P* species a Method 2 was used to analyze P and P*. In this
317 case, the cross flow gradient is lowered from 0.8 ml/min to 0.3 ml/min (starting rate) to ease the
318 separation and elution of the hydrodynamically bigger species uncovered with Method 1.

319 With this second method, the oligomeric species of standard phaseolin cannot be resolved anymore,
320 and P is eluted as a single peak at 10 min (Figure 6, panel a). The corresponding calculated molar
321 mass (263 kDa) confirms that the peak is indeed a mixture of trimer and heavier species.

322 On the other hand, P* shows the presence of trace of oligomers (Figure 6b) with a peak at 8 minutes
323 (in common with P), but is mainly composed of two heavier species which resulted now distinct.

324 The first was eluted with a maximum at 14 minutes, and a molar mass averaging at 0.8×10^6 Da,
325 while the second is even heavier and reaches 10^7 Da. However, it is not clear how P* monomers are
326 organized in these two distinct high-molecular weight (HMW) polymeric species.

327 One indication on the conformation state of mutated phaseolin HMW-forms can be offered with the
328 calculation of their shape factor. When considering an eluting band, the corresponding molar mass
329 and RMS radius (from light scattering characterization) can be plotted in the logarithmic form to
330 obtain a slope (v value) related to conformation. Generally, a value of 0.33 corresponds to a solid
331 sphere, while higher values indicate a less compact or elongated structure like a random coil (0.5) or
332 a rod (1) [51], [52], [53].

333 In the case of standard phaseolin, the oligomeric forms are compact, as the 0.26 v value suggests
334 (Table 3).

335 This is in line with the aggregation model of phaseolin, which envisions a triangular assembly [54].
336 Instead, different values emerge for P* higher order species, which rather denote the formation of
337 random coils (Band 2) and more extended shapes (Band 3). This supports the idea of the successful
338 polymerization of P* caused by its mutation, which prevents the conventional 3-unit aggregation and
339 favours the concatenation of more units by means of disulfide bonds.

340
341
342
343
344
345
346
347
348
349
350
351
352
353
354
355
356
357
358
359
360
361
362
363
364

4. Conclusions

The use of protein biopolymers for film production is very appealing, given their excellent properties and their potential in replacing fossil-fuel plastics. Moreover, plant-based proteins can represent a sustainable source and are of great interest. [55]

In this work, we employed a combination of hollow-fiber flow field flow fractionation methods combined to UV and MALS detection, to identify and characterize polymeric forms of P*, a mutated protein obtained from the thylakoid compartment of transplastomic tobacco plants.

Protein extracts derived from *P. vulgaris* showed the presence of native phaseolin, prevalently as trimer, while there was no evidence of polymeric forms, as expected. When extracts from tobacco were instead analyzed, we found evidence of higher molar mass species, and traces of oligomeric phaseolin. Moreover, the high molecular weight (HMW) species, characterized using a second separation method, were two and distinct, one averaging 0.8×10^6 Da and the second reaching the tens of million Da. Insight of the conformation of these HMW species was offered from their v values, which corresponded to those of coils and longer chain structures, confirming the positive impact of the Cys modification on polymerization.

The HF5-UV-MALS system was successful in evaluating the different aggregation status of native phaseolin and monitoring the formation of two distinct polymeric species in modified P*. **The approach will be useful in assisting the further optimization steps of this process.** The formation of phaseolin polymers in chloroplasts, not present in *P. vulgaris*, could be very interesting for industrial purposes. Chloroplasts from cultivated transplastomic tobacco plants could be employed as a reactor to produce a biopolymer derived from an edible protein, with a possible application in the production of biodegradable films.

365 **References**

366

- 367 1. Pathak, S., C. Sneha, and B.B. Mathew, *Bioplastics: Its Timeline Based Scenario & Challenges*.
368 Journal of Polymer and Biopolymer Physics Chemistry, 2014. **2**(4): p. 84-90.
- 369 2. Calva-Estrada, S.J., M. Jiménez-Fernández, and E. Lugo-Cervantes, *Protein-Based Films: Advances in*
370 *the Development of Biomaterials Applicable to Food Packaging*. Food Engineering Reviews, 2019.
371 **11**(2): p. 78-92.
- 372 3. Bhawani, S.A., et al., *Proteins as Agricultural Polymers for Packaging Production*, in
373 *Bionanocomposites for Packaging Applications*, M. Jawaid and S.K. Swain, Editors. 2018, Springer
374 International Publishing: Cham. p. 243-267.
- 375 4. Sun, S.M., et al., *Protein Synthesis and Accumulation in Bean Cotyledons during Growth*. Plant
376 Physiology, 1978. **61**(6): p. 918-923.
- 377 5. Nedumaran, S., et al. *Grain Legumes Production, Consumption and Trade Trends in Developing*
378 *Countries-An Assessment & Synthesis*. 2019.
- 379 6. Lawrence, M.C., et al., *Structure of Phaseolin at 2.2 Å Resolution: Implications for a Common*
380 *Vicilin/Legumin Structure and the Genetic Engineering of Seed Storage Proteins*. Journal of Molecular
381 Biology, 1994. **238**(5): p. 748-776.
- 382 7. Lawrence, M.C., et al., *The three-dimensional structure of the seed storage protein phaseolin at 3 Å*
383 *resolution*. The EMBO journal, 1990. **9**(1): p. 9-15.
- 384 8. Slightom, J.L., et al., *Nucleotide sequences from phaseolin cDNA clones: the major storage proteins*
385 *from Phaseolus vulgaris are encoded by two unique gene families*. Nucleic acids research, 1985.
386 **13**(18): p. 6483-6498.
- 387 9. Yin, S.-W., et al., *Functional and conformational properties of phaseolin (Phaseolus vulgris L.) and*
388 *kidney bean protein isolate: A comparative study*. Journal of the Science of Food and Agriculture,
389 2010. **90**(4): p. 599-607.
- 390 10. Yin, S.-W., et al., *Surface charge and conformational properties of phaseolin, the major globulin in*
391 *red kidney bean (Phaseolus vulgaris L): effect of pH*. International Journal of Food Science &
392 Technology, 2011. **46**(8): p. 1628-1635.
- 393 11. de Virgilio, M., et al., *The human immunodeficiency virus antigen Nef forms protein bodies in leaves*
394 *of transgenic tobacco when fused to zeolin*. Journal of experimental botany, 2008. **59**(10): p. 2815-
395 2829.
- 396 12. De Marchis, F., A. Pompa, and M. Bellucci, *Plastid Proteostasis and Heterologous Protein*
397 *Accumulation in Transplastomic Plants*. Plant Physiology, 2012. **160**(2): p. 571-581.
- 398 13. Fuentes, P., T. Armarego-Marriott, and R. Bock, *Plastid transformation and its application in*
399 *metabolic engineering*. Current Opinion in Biotechnology, 2018. **49**: p. 10-15.
- 400 14. Guda, C., S.B. Lee, and H. Daniell, *Stable expression of a biodegradable protein-based polymer in*
401 *tobacco chloroplasts*. Plant Cell Reports, 2000. **19**(3): p. 257-262.
- 402 15. Chebolu, S. and H. Daniell, *Chloroplast-derived vaccine antigens and biopharmaceuticals: expression,*
403 *folding, assembly and functionality*. Current topics in microbiology and immunology, 2009. **332**: p.
404 33-54.
- 405 16. Pompa, A., et al., *An engineered C-terminal disulfide bond can partially replace the phaseolin vacuolar*
406 *sorting signal*. The Plant Journal, 2010. **61**(5): p. 782-791.
- 407 17. De Marchis, F., et al., *A plant secretory signal peptide targets plastome-encoded recombinant*
408 *proteins to the thylakoid membrane*. Plant Molecular Biology, 2011. **76**(3): p. 427-441.
- 409 18. De Marchis, F., M. Bellucci, and A. Pompa, *Phaseolin expression in tobacco chloroplast reveals an*
410 *autoregulatory mechanism in heterologous protein translation*. Plant Biotechnology Journal, 2016.
411 **14**(2): p. 603-614.
- 412 19. *FDA Guidance for Industry: Immunogenicity-Related Considerations for Low Molecular Weight*
413 *Heparin*
- 414 20. Giddings, J., *Field-flow fractionation: analysis of macromolecular, colloidal, and particulate materials*.
415 Science, 1993. **260**(5113): p. 1456-1465.

- 416 21. Zattoni, A., et al., *Asymmetrical flow field-flow fractionation with multi-angle light scattering*
417 *detection for the analysis of structured nanoparticles*. Journal of Chromatography A, 2009. **1216**(52):
418 p. 9106-9112.
- 419 22. Tanase, M., et al., *Hydrodynamic size-based separation and characterization of protein aggregates*
420 *from total cell lysates*. Nature protocols, 2015. **10**(1): p. 134-148.
- 421 23. Reschiglian, P., et al., *Hollow-fiber flow field-flow fractionation with multi-angle laser scattering*
422 *detection for aggregation studies of therapeutic proteins*. Analytical and Bioanalytical Chemistry,
423 2014. **406**(6): p. 1619-1627.
- 424 24. Marassi, V., et al., *A new approach for the separation, characterization and testing of potential*
425 *prionoid protein aggregates through hollow-fiber flow field-flow fractionation and multi-angle light*
426 *scattering*. Analytica Chimica Acta, 2019. **1087**: p. 121-130.
- 427 25. Fuentes, C., et al., *Characterization of molecular properties of wheat starch from three different types*
428 *of breads using asymmetric flow field-flow fractionation (AF4)*. Food Chemistry, 2019. **298**: p. 125090.
- 429 26. Wu, D.-T., et al., *Molecular characterization of branched polysaccharides from Tremella fuciformis by*
430 *asymmetrical flow field-flow fractionation and size exclusion chromatography*. Journal of Separation
431 Science, 2017. **40**(21): p. 4272-4280.
- 432 27. Lu, Y., B. Bergenståhl, and L. Nilsson, *Interfacial properties and interaction between beer wort protein*
433 *fractions and iso-humulone*. Food Hydrocolloids, 2020. **103**: p. 105648.
- 434 28. Marassi, V., et al., *Characterization of red wine native colloids by asymmetrical flow field-flow*
435 *fractionation with online multidetection*. Food Hydrocolloids, 2021. **110**: p. 106204.
- 436 29. Coelho, C., et al., *Asymmetrical flow field-flow fractionation of white wine chromophoric colloidal*
437 *matter*. Analytical and Bioanalytical Chemistry, 2017. **409**(10): p. 2757-2766.
- 438 30. Pitkänen, L., P. Tuomainen, and K. Eskelin, *Analysis of plant ribosomes with asymmetric flow field-*
439 *flow fractionation*. Anal Bioanal Chem, 2014. **406**(6): p. 1629-37.
- 440 31. Marassi, V., et al., *Hollow fiber flow field-flow fractionation and size-exclusion chromatography with*
441 *multi-angle light scattering detection: A complementary approach in biopharmaceutical industry*.
442 Journal of Chromatography A, 2014. **1372**: p. 196-203.
- 443 32. Andrea, Z., et al., *Hollow-Fiber Flow Field-Flow Fractionation*. Current Analytical Chemistry, 2007.
444 **3**(4): p. 310-323.
- 445 33. Reschiglian, P., et al., *On-Line Hollow-Fiber Flow Field-Flow Fractionation-Electrospray*
446 *Ionization/Time-of-Flight Mass Spectrometry of Intact Proteins*. Analytical Chemistry, 2005. **77**(1): p.
447 47-56.
- 448 34. Zattoni, A., et al., *Hollow-fiber flow field-flow fractionation of whole blood serum*. Journal of
449 Chromatography A, 2008. **1183**(1): p. 135-142.
- 450 35. Johann, C., et al., *A novel approach to improve operation and performance in flow field-flow*
451 *fractionation*. Journal of Chromatography A, 2011. **1218**(27): p. 4126-4131.
- 452 36. Rambaldi, D.C., et al., *In vitro amyloid Aβ1-42 peptide aggregation monitoring by asymmetrical flow*
453 *field-flow fractionation with multi-angle light scattering detection*. Analytical and Bioanalytical
454 Chemistry, 2009. **394**(8): p. 2145-2149.
- 455 37. Reschiglian, P., et al., *Hollow-Fiber Flow Field-Flow Fractionation: A Pipeline to Scale Down Separation*
456 *and Enhance Detection of Proteins and Cells*, in *Field-Flow Fractionation in Biopolymer Analysis*, S.K.R.
457 Williams and K.D. Caldwell, Editors. 2012, Springer Vienna: Vienna. p. 37-55.
- 458 38. Zattoni, A., et al., *Hollow-fiber flow field-flow fractionation: a novel pre-MS method for proteomics*.
459 Journal of Biotechnology, 2010. **150**: p. 207-208.
- 460 39. Pedrazzini, E., et al., *Protein quality control along the route to the plant vacuole*. The Plant cell, 1997.
461 **9**(10): p. 1869-1880.
- 462 40. Watson, J., et al., *Expression of Bacillus anthracis protective antigen in transgenic chloroplasts of*
463 *tobacco, a non-food/feed crop*. Vaccine, 2004. **22**(31): p. 4374-4384.
- 464 41. Dhingra, A., A.R. Portis, and H. Daniell, *Enhanced translation of a chloroplast-expressed*
465 *RbcS gene restores small subunit levels and photosynthesis in nuclear RbcS*
466 *antisense plants*. Proceedings of the National Academy of Sciences of the United States of America,
467 2004. **101**(16): p. 6315-6320.

- 468 42. Bellucci, M., et al., *A mutant Synechococcus gene encoding glutamate 1-semialdehyde*
469 *aminotransferase confers gabaculine resistance when expressed in tobacco plastids*. Plant Cell
470 Reports, 2015. **34**(12): p. 2127-2136.
- 471 43. Suzuki, E., et al., *Crystallization of phaseolin from Phaseolus vulgaris*. Journal of Biological Chemistry,
472 1983. **258**(4): p. 2634-6.
- 473 44. Bellucci, M., et al., *Accumulation of maize γ -zein and γ -zein: KDEL to high levels in tobacco leaves and*
474 *differential increase of BiP synthesis in transformants*. Theoretical and Applied Genetics, 2000.
475 **101**(5): p. 796-804.
- 476 45. Beckett, R., Z. Jue, and J.C. Giddings, *Determination of molecular weight distributions of fulvic and*
477 *humic acids using flow field-flow fractionation*. Environmental Science & Technology, 1987. **21**(3): p.
478 289-295.
- 479 46. Marassi, V., et al., *Hollow-fiber flow field-flow fractionation and multi-angle light scattering as a new*
480 *analytical solution for quality control in pharmaceutical nanotechnology*. Microchemical Journal,
481 2018. **136**: p. 149-156.
- 482 47. Striegel, A.M., *Stapan Podzimek: Light scattering, size exclusion chromatography and asymmetric*
483 *flow field flow fractionation. Powerful tools for the characterization of polymers, proteins and*
484 *nanoparticles*. Analytical and Bioanalytical Chemistry, 2012. **402**(5): p. 1857-1858.
- 485 48. Masuelli, M. and D. Renard, *Advances in Physicochemical Properties of Biopolymers (Part 1)*. 2017:
486 Bentham Science Publishers.
- 487 49. Bollini, R., A. Vitale, and M.J. Chrispeels, *In vivo and in vitro processing of seed reserve protein in the*
488 *endoplasmic reticulum: evidence for two glycosylation steps*. The Journal of cell biology, 1983. **96**(4):
489 p. 999-1007.
- 490 50. Blagrove, R.J., et al., *Physicochemical and structural studies of phaseolin from French bean seed*. Plant
491 Foods for Human Nutrition, 1983. **33**(2): p. 227-229.
- 492 51. Smilgies, D.-M. and E. Folta-Stogniew, *Molecular weight-rotation radius relation of globular proteins:*
493 *a comparison of light scattering, small-angle X-ray scattering and structure-based data*. Journal of
494 applied crystallography, 2015. **48**(Pt 5): p. 1604-1606.
- 495 52. Corporation, W.T.; Available from: [https://www.wyatt.com/solutions/properties/conformation-of-](https://www.wyatt.com/solutions/properties/conformation-of-macromolecules-and-nanoparticles.html)
496 [macromolecules-and-nanoparticles.html](https://www.wyatt.com/solutions/properties/conformation-of-macromolecules-and-nanoparticles.html).
- 497 53. Feroz Jameel, S.H., *Formulation and Process Development Strategies for Manufacturing*
498 *Biopharmaceuticals*.
- 499 54. Foresti, O., et al., *A phaseolin domain involved directly in trimer assembly is a determinant for binding*
500 *by the chaperone BiP*. Plant Cell, 2003. **15**(10): p. 2464-75.
- 501 55. Chen, H., et al., *Application of Protein-Based Films and Coatings for Food Packaging: A Review*.
502 Polymers (Basel), 2019. **11**(12).

503

504

505 **Figure captions**

506

507 **Figure 1.** Localization of Modified Phaseolin (P^*) localization in transplastomic chloroplast
508 compartments (thylakoids) of tobacco leaves.

509

510 **Figure 2:** (A) SDS-PAGE stained by Coomassie of P (0.5 μg) extracted from *P. vulgaris* (left) and
511 Western blot of the same P (0.04 μg) sample using anti-phaseolin antiserum (right). Arrows indicate
512 differentially glycosylated monomers of α - and β -phaseolin, (B) Total proteins (20 μg) extracted from
513 leaves of transplastomic plants expressing P^* and P (0.06 μg) extracted from *P. vulgaris* were
514 analysed by Western blotting with anti-phaseolin antiserum. Due to the higher amount of protein
515 loaded in the Western blot in (b) with respect to that in (a), phaseolin in the P sample migrated
516 apparently as a single band, instead of three bands of α - and β -polypeptides as in (a). Black
517 arrowhead indicates the mutated β -phaseolin monomer (P^*) at 45 kDa, white arrowhead indicates
518 P^* dimers, and brace indicates P^* high-molecular mass forms unresolved by SDS page. Numbers on
519 the left of the figures indicate the positions of molecular mass markers in kDa.

520

521 **Figure 3:** (a) Schematic representation of P^* purification that is described in detail in the Materials
522 and methods section. (b) Each fraction and the pellet (indicated at the top) obtained from the velocity
523 Suc gradient (a) analyzed by protein blot and visualized using anti-phaseolin antiserum. At the
524 bottom, numbers indicate molecular mass of sedimentation markers (kDa) and the Suc concentration
525 of the fractions is shown. Black arrowhead indicates P^* monomers, white arrowhead indicates P^*
526 dimers, and brace indicates P^* high-molecular mass forms.

527

528 **Figure 4.** Separation profile (grey, UV@280 nm) and molar mass calculation (green) of P
529 characterization with the first method

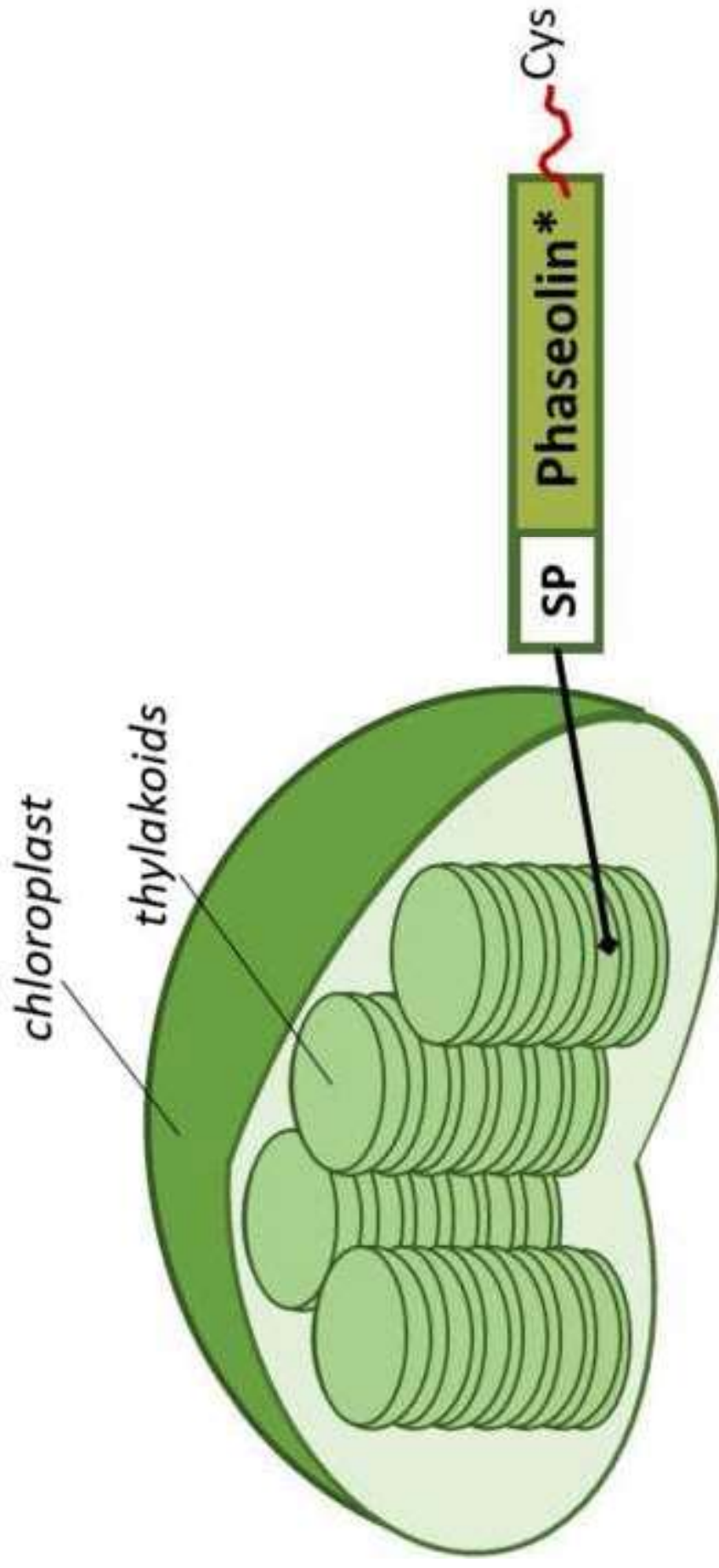
530

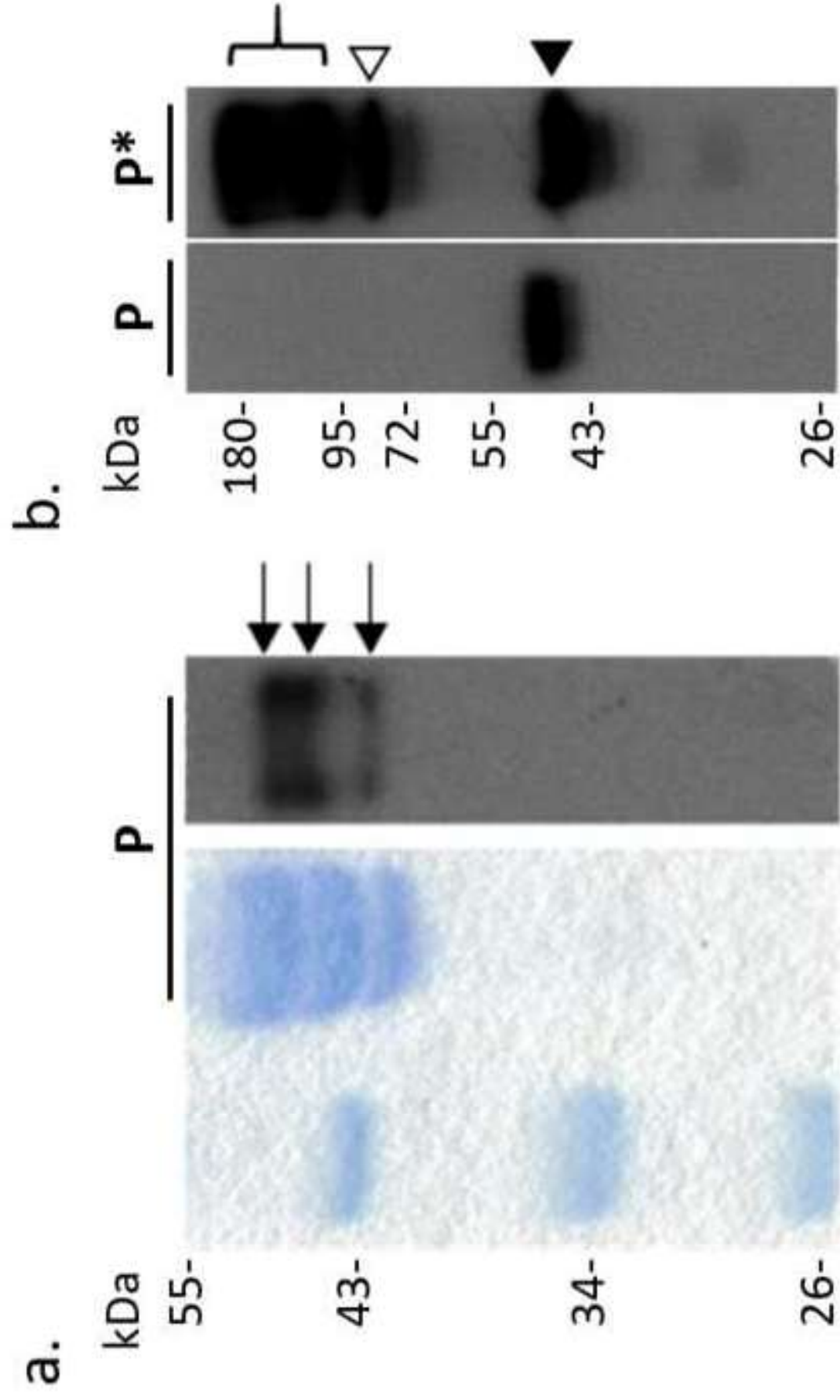
531 **Figure 5.** Separation profile (grey, UV@280 nm) and molar mass calculation (green) of P^*
532 characterization with the first method

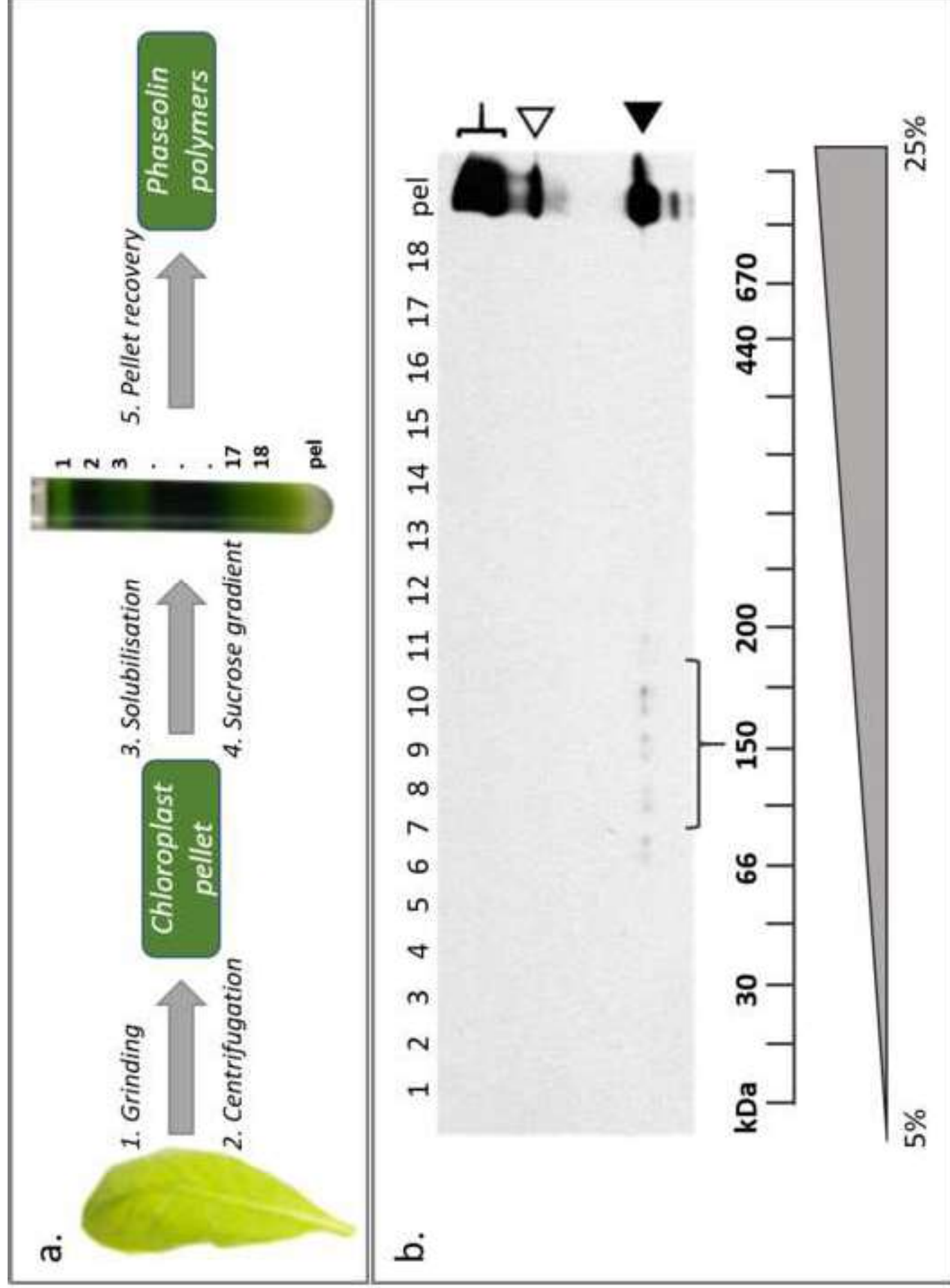
533

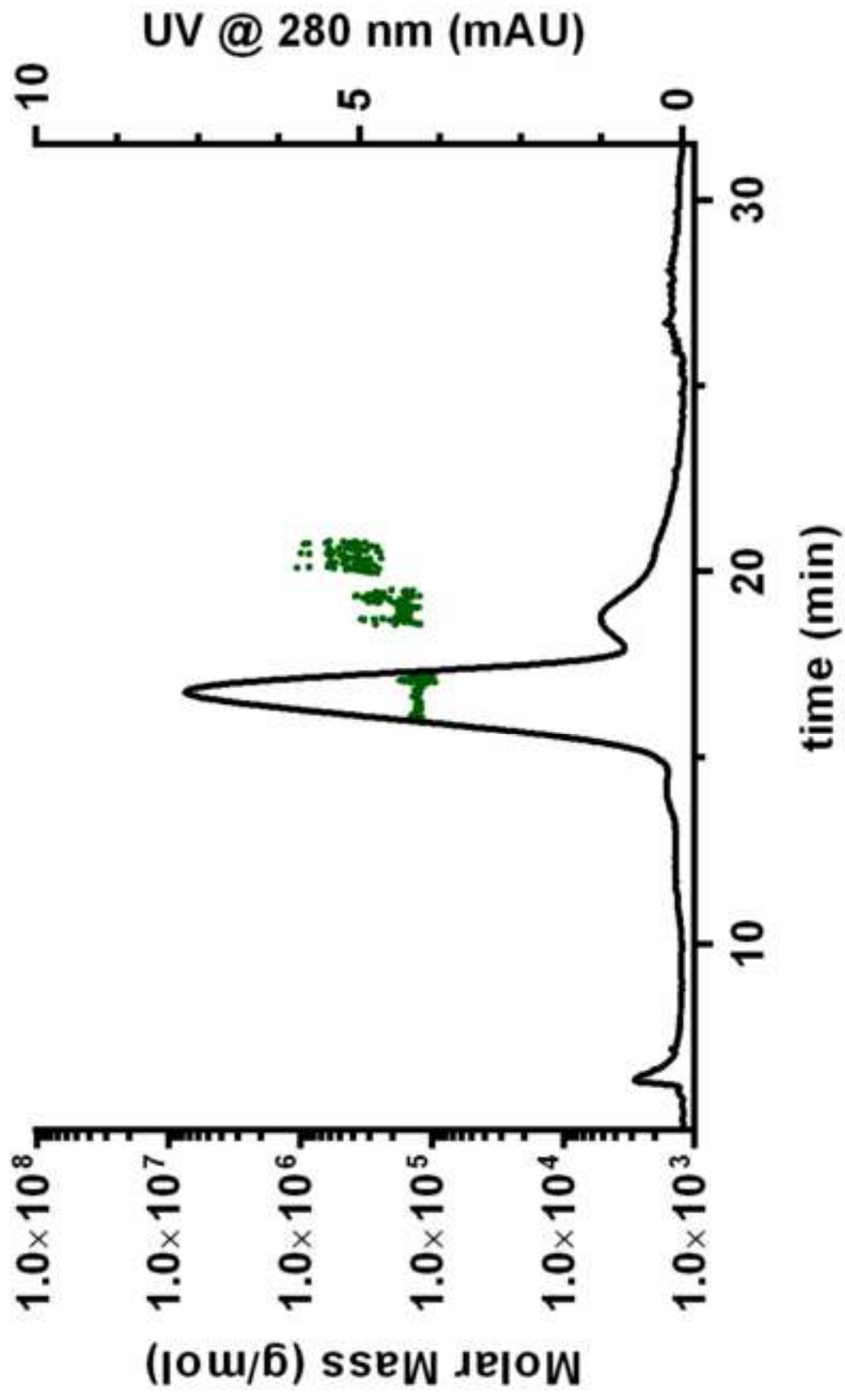
534 **Figure 6.** Fractogram (grey, UV@280 nm) and molar mass calculation (green) of (a) P
535 characterization and (b) P^* characterization with the Method 2.

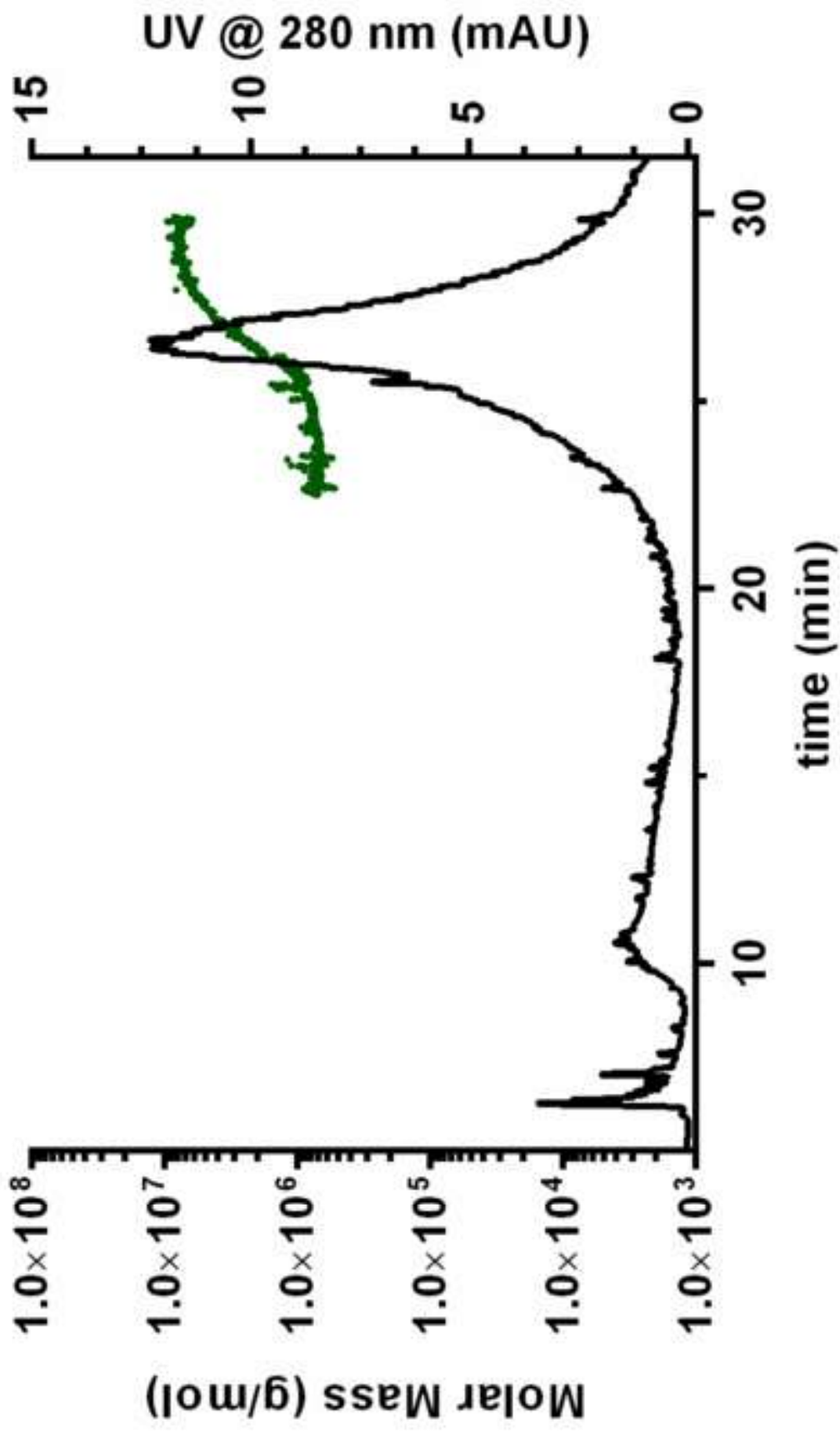
536

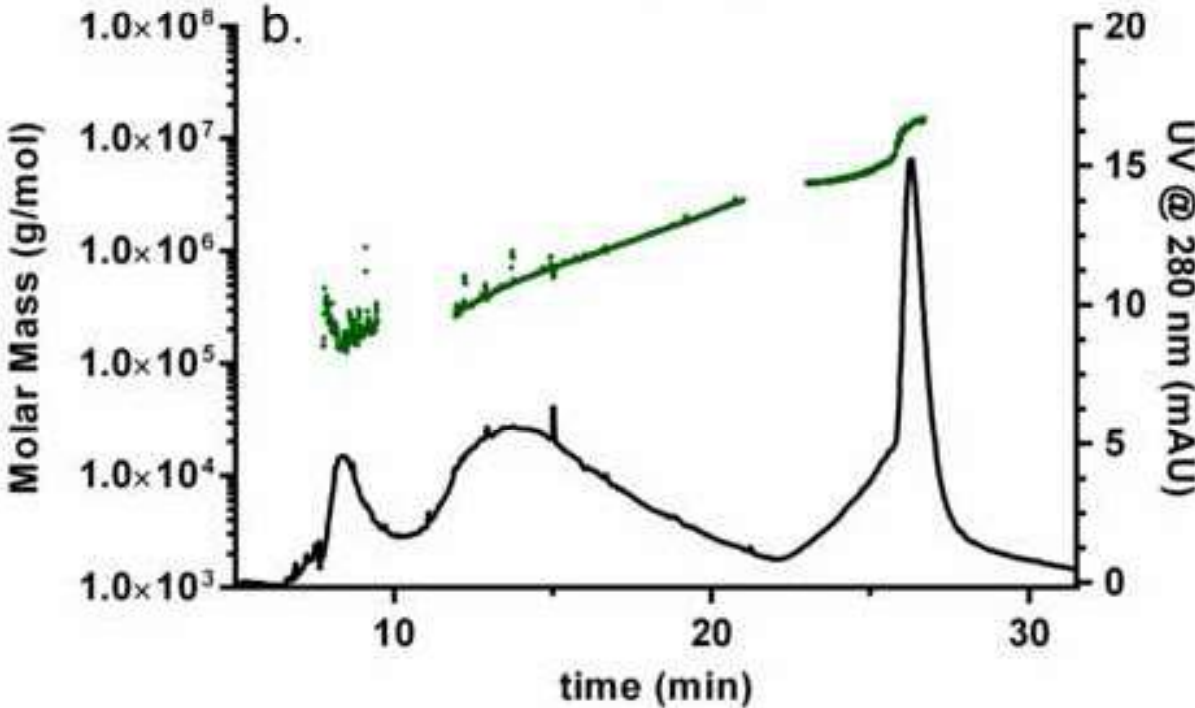
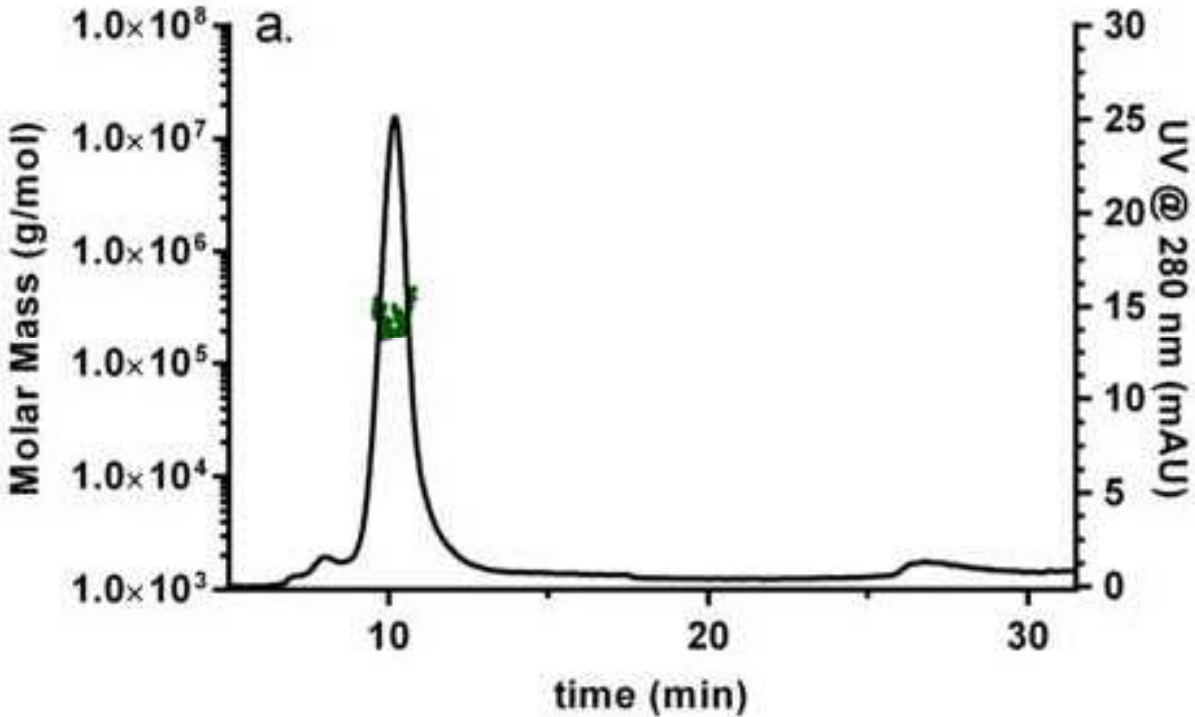












| Steps → ↓Method | Focus (mL/min) | Focus- injection (mL/min) | Elution (mL/min) | | | | Elution-Inject (mL/min) |
|--------------------------------|---|---|---|---|--|--|--|
| | | | | | | | |
| Phaseolin characterisation | V _c =0.25 V _x =0.80 Time=0.5 min | V _c =0.25 V _x =0.80 Time=5 min | V _c =0.25 V _x =0.80 to 0.03 Time=20 min | | V _c =0.25 V _x =0 Time=5 min | | V _c =0.25 V _x =0 Time =3 min |
| Aggregates Characterisation | V _c =0.35 V _x =0.80 Time=0.5 min | V _c =0.35 V _x =0.80 Time=5 min | V _c =0.35 V _x =0.30 to 0.1 Time=5 min | V _c =0.35 V _x =0.1 Time=10 min | V _c =0.35 V _x =0.1 to 0.0 Time=5 min | V _c =0.35 V _x =0.0 Time=5 min | V _c =0.35 V _x =0 Time =3 min |

Table 1. Flow conditions for HF5 analyses

| Peaks → Characterisation ↓ | Min 14 | Min 16.5 | Min 19 | Min 21 |
|-------------------------------|--------|----------|--------|--------|
| % area | 3% | 78% | 10% | 9% |
| Peak attribution | 2-mer | 3-mer | 6-mer | 9-mer |

Table 2. Phaseolin aggregation states

| Shape factor of species (v value) | Band 1 (9.5 to 11 minutes) | Band 2 (13 to 17 minutes) | Band 3 (23 to 26 minutes) |
|--------------------------------------|-------------------------------|------------------------------|------------------------------|
| Standard phaseolin | 0.26 ± 0.01 | - | - |
| Mutated P* | - | 0.52 ± 0.09 | 0.8 ± 0.02 |

Table 3. Shape factors of phaseolin and mutated phaseolin (P*) bands obtained from method 2.

Authors Credit role

Valentina Marassi: formal analysis; methodology; data curation; Roles/Writing - original draft

Francesca De Marchis: Conceptualization; data curation; Roles/Writing - original draft; Writing - review & editing

Barbara Roda: Resources; Writing - review & editing

Michele Bellucci: Conceptualization; data curation; Roles/Writing - original draft; Writing - review & editing

Alice Capecchi: formal analysis; methodology; data curation

Pierluigi Reschiglian: Funding acquisition; Writing - review & editing

Andrea Pompa: Conceptualization; data curation; Roles/Writing - original draft; Writing - review & editing

Andrea Zattoni: Conceptualization; methodology; data curation; Roles/Writing - original draft; Writing - review & editing

Declaration of interests

- The authors declare that they have no known competing financial interests or personal relationships that could have appeared to influence the work reported in this paper.
- The authors declare the following financial interests/personal relationships which may be considered as potential competing interests:

V. Marassi, B. Roda, P. Reschiglian and A. Zattoni are associates of the academic spinoff company byFlow Srl (Bologna, Italy). The company mission includes know-how transfer, development, and application of novel technologies and methodologies for the analysis and characterization of samples of nano-biotechnological interest.